https://doi.org/10.5194/egusphere-2026-1362
Preprint. Discussion started: 11 May 2026

Consistent ridging and opening coefficients for multi-category sea ice models with modified viscous-plastic rheologies

Jean-François Lemieux[1], Damien Ringeisen[2], Martin Losch[3], William H. Lipscomb[4], and Jinro Ukita[5]

[1]Recherche en Prévision Numérique Environnementale, Environnement et Changement Climatique Canada, 2121 route Transcanadienne, Dorval QC, Canada.
[2]Canadian Centre for Climate Modelling and Analysis, Climate Research Division, Environment and Climate Change Canada, Victoria, BC, Canada.
[3]Alfred-Wegener-Institut, Helmholtz-Zentrum für Polar- und Meeresforschung, Bremerhaven, Germany.
[4]Climate and Global Dynamics Laboratory, NSF National Center for Atmospheric Research, Boulder, CO, USA.
[5]Meteorological Research Institute, Japan Meteorological Agency, Tsukuba, Japan.

Correspondence: Jean-François Lemieux (jean-francois.lemieux@ec.gc.ca)

Abstract.

In multi-thickness category sea ice models, subgrid-scale ridging and the opening of leads are represented by a redistribution function. This function modifies the thickness distribution based on grid-scale strain rates. There is a physical link between sea ice rheology and redistribution by assuming that the work done by internal stresses in deforming sea ice is equal to the change in potential energy and frictional loss during the formation of ridges. Hence, modifications of the rheology require changes to the redistribution function to be consistent. For the special case of an elliptical yield curve and a non-normal flow rule, associated consistent ridging and opening coefficients can be formulated such that they reduce to the standard ones in the case of a normal flow rule. It is further demonstrated that the coefficients are independent of biaxial tensile strength. Satisfying specific criteria for the yield curve and plastic potential aspect ratios ensures that the ridging and opening coefficients are bounded by 0 and 1.

1 Introduction

Many physical processes in sea ice depend on sea ice thickness. For example, the thermodynamical growth rate over thin ice can be more than one order of magnitude larger than over thick ice, and the compressive ice strength depends strongly on the amount of thin ice and open water in a given region. This is why most continuum-based sea ice models now use an ice thickness distribution (ITD) to represent the fractions of different thicknesses present in a grid cell. The ITD evolves due to thermodynamical growth and melt, advection, and mechanical redistribution.

https://doi.org/10.5194/egusphere-2026-1362
Preprint. Discussion started: 11 May 2026

The mechanical redistribution function is an important term of the equation describing the evolution of the ITD (Thorndike et al., 1975). Given grid-scale strain rates, this function redistributes volume among the thickness categories to represent the subgrid-scale ridging and opening processes. Thicknesses are redistributed by the ridging and opening modes with relative contributions determined by so-called ridging and opening coefficients. In this article, we do not modify the ridging and opening modes but derive consistent ridging and opening coefficients for modified viscous-plastic (VP) rheologies.

VP rheologies are characterized by a yield curve and a flow rule. The yield curve defines critical stresses. When the state of stress is inside the yield curve, sea ice behaves as a very viscous, nearly rigid material, but when the stresses reach the yield curve, the ice can undergo large plastic deformations. The flow rule determines the relative amount of divergence and shear for a given point on the yield curve. The yield curve, the flow rule, and the redistribution function are related when assuming that the work done during ridging is equal to the change in potential energy and frictional loss (Coon et al., 1974; Rothrock, 1975).

It is impossible to measure large-scale stresses and very difficult to simultaneously observe small-scale ridging, opening and sliding events, and the large-scale strain rates. Thus, sea ice rheology and mechanical redistribution rely on many assumptions and are the subject of active research. There are two approaches to relate the redistribution function and the rheology. In the first approach, a yield curve is derived based on assumptions for the ridging, opening and sliding processes (e.g., Ukita and Moritz, 1995; Moritz and Ukita, 2000; Wilchinsky et al., 2006). In the second approach, ridging and opening coefficients are obtained after defining a yield curve and a flow rule (e.g., Stern et al., 1995; Lipscomb et al., 2007). This is the approach taken in this article. Note that, as the subgrid-scale sliding does not redistribute thicknesses (Wilchinsky et al., 2006), a formulation for the sliding coefficient is not required in this case.

Using grid-scale strain rates, the relative amount of ridging and opening are expressed by the ridging and opening coefficients, which should vary between 0 and 1. Given a yield curve and a flow rule, the ridging and opening coefficients can be derived. The standard VP rheology has a normal flow rule and an elliptical yield curve with zero tensile strength (Hibler, 1979). Many continuum-based sea ice models have implemented formulations of the opening and ridging coefficients that are consistent with the standard VP rheology (e.g., CICE, Lipscomb et al., 2007).

In recent years, however, modifications to the standard VP rheology have been introduced. Using a VP constitutive equation that allows sea ice to resist additional biaxial tensile stress (König Beatty and Holland, 2010) can improve the simulation of landfast ice in regions such as the Kara Sea (with CICE, Lemieux et al., 2016). Other community models obtained similar results with added tensile strength (MITgcm, LIM/SI3, Itkin et al., 2015; Van Achter et al., 2022). Adding a plastic potential that defines the flow rule independently from the yield curve leads to a VP rheology with a non-normal flow rule, with properties distinctly different from the standard model (Ringeisen et al., 2021).

The main contribution of this article is to derive consistent ridging and opening coefficients for modified VP rheologies with elliptical yield curves, specifically with additional tensile strength and a non-normal flow rule. The plastic potential is here also

https://doi.org/10.5194/egusphere-2026-1362
Preprint. Discussion started: 11 May 2026

defined by an ellipse. Another interesting outcome of this study is the determination of the range of yield curve and plastic potential aspect ratios that lead to realistic ridging and opening coefficients (i.e., bounded by 0 and 1).

This article is structured as follows. Section 2 introduces the redistribution function, the ridging and opening modes, and the ridging and opening coefficients for the VP elliptical yield curve with a normal flow rule. Section 3 derives the ridging and opening coefficients for modified VP rheologies, and Sect. 4 provides the range of valid values of the aspect ratios for the yield curve and plastic potential. Section 5 contrasts the new formulation with two possible incorrect formulations of the coefficients. The numerical experiments and the main results are presented in Section 6 and 7. Section 8 includes a discussion and concluding remarks.

2 The mechanical redistribution function

We give here a brief overview of the redistribution function and introduce useful variables for the rest of this article. Following Thorndike et al. (1975), the redistribution function is expressed as

$$\psi = |\dot{\epsilon}| \left[\alpha_o(\theta)\omega_o + \alpha_r(\theta)\omega_r\right], \tag{1}$$

where $|\dot{\epsilon}| = (\dot{\epsilon_{\rm I}}^2 + \dot{\epsilon_{\rm II}}^2)^{1/2}$ with the strain rate invariants $\dot{\epsilon_{\rm I}}$ (divergence) and $\dot{\epsilon_{\rm II}}$ (shear). ω_o is the opening mode, ω_r is the ridging mode, and $\alpha_o(\theta)$ and $\alpha_r(\theta)$ are the opening and ridging coefficients. These coefficients depend on the angle $\theta = \tan^{-1}(\dot{\epsilon_{\rm II}}/\dot{\epsilon_{\rm I}})$, which is a measure of the relative amount of shear and divergence.

The opening mode ω_o is expressed with the delta function $\delta(h)$ where h is the sea ice thickness. The role of this mode is to represent subgrid-scale opening events by modifying the areal fraction of open water. Thorndike et al. (1975) introduced the more complicated ridging mode ω_r. The formulation of ω_r used in CICE is described in Lipscomb et al. (2007).

The ridging and opening coefficients for the VP rheology with an elliptical yield curve, no tensile strength, and a normal flow rule are given by Stern et al. (1995) and Lipscomb et al. (2007). Following Lipscomb et al. (2007), the ridging coefficient can be expressed as a function of the strain rates as

$$\alpha_r(\theta) = \frac{1}{2|\dot{\epsilon}|}\left[\Delta - \dot{\epsilon_{\rm I}}\right], \tag{2}$$

where $\Delta = [\dot{\epsilon_{\rm I}}^2 + e^{-2}\dot{\epsilon_{\rm II}}^2]^{1/2}$ with e the aspect ratio of the elliptical yield curve (Hibler, 1979).

Given the ridging coefficient in Eq. (2), the opening coefficient can then simply be obtained as $\alpha_o(\theta) = \alpha_r(\theta) + \cos\theta$ (Thorndike et al., 1975).

https://doi.org/10.5194/egusphere-2026-1362
Preprint. Discussion started: 11 May 2026

3 Ridging and opening coefficients for modified rheologies

3.1 Coefficients for a non-normal flow rule

Stern et al. (1995) derived the ridging and opening coefficients for a VP rheology with an elliptical yield curve, no tensile strength, and a normal flow rule (Hibler, 1979). We refer to this as the standard VP rheology. We wish here to derive a more general formulation that is consistent with an elliptical yield curve and an elliptical plastic potential allowing a non-normal flow rule (Ringeisen et al., 2021). We defer the discussion of tensile strength to the next section.

Eq. (14) in Rothrock (1975) equates the work done during ridging to the potential energy production and frictional energy loss. It is expressed as

$$\sigma_{\mathrm{I}}\dot{\epsilon_{\mathrm{I}}} + \sigma_{\mathrm{II}}\dot{\epsilon_{\mathrm{II}}} = |\dot{\epsilon}|\alpha_r(\theta)P_r, \tag{3}$$

where σ_{I} and σ_{II} are the stress invariants and P_r is the ice strength in compression. The derivations below assume that tensile strength is zero and that the sea ice stresses are in the plastic regime, that is, on the yield curve.

The stress invariants are given by

$$\sigma_{\mathrm{I}} = \zeta\dot{\epsilon_{\mathrm{I}}} - \frac{P_r}{2}, \tag{4}$$

$$\sigma_{\mathrm{II}} = \eta\dot{\epsilon_{\mathrm{II}}}, \tag{5}$$

where ζ is the bulk viscosity and η is the shear viscosity.

Given e_{F} and e_{G}, the ellipse aspect ratios for the yield curve and the plastic potential, ζ and η are given by

$$\zeta = \frac{P_r}{2\Delta_{\mathrm{FG}}}, \tag{6}$$

$$\eta = e_{\mathrm{G}}^{-2}\zeta, \tag{7}$$

where $\Delta_{\mathrm{FG}} = [\dot{\epsilon_{\mathrm{I}}}^2 + e_{\mathrm{F}}^2 e_{\mathrm{G}}^{-4}\dot{\epsilon_{\mathrm{II}}}^2]^{1/2}$ (Ringeisen et al., 2021). The subscript FG indicates that Δ_{FG} is a function of e_{F} and e_{G}.

Using Eqs. (4) and (5), Eq. (3) can be written as

$$\zeta\dot{\epsilon_{\mathrm{I}}}^2 - \frac{P_r}{2}\dot{\epsilon_{\mathrm{I}}} + \eta\dot{\epsilon_{\mathrm{II}}}^2 = |\dot{\epsilon}|\alpha_r(\theta)P_r. \tag{8}$$

Replacing the viscosities in Eq. (8) by Eqs. (6) and (7) we obtain

$$\frac{P_r}{2\Delta_{\mathrm{FG}}}\dot{\epsilon_{\mathrm{I}}}^2 - \frac{P_r}{2}\dot{\epsilon_{\mathrm{I}}} + \frac{e_{\mathrm{G}}^{-2}P_r}{2\Delta_{\mathrm{FG}}}\dot{\epsilon_{\mathrm{II}}}^2 = |\dot{\epsilon}|\alpha_r(\theta)P_r, \tag{9}$$

https://doi.org/10.5194/egusphere-2026-1362
Preprint. Discussion started: 11 May 2026

which can be rearranged as

$$\alpha_r(\theta) = \frac{1}{2|\dot{\epsilon}|}\left[\frac{1}{\Delta_{\mathrm{FG}}}(\dot{\epsilon_{\mathrm{I}}}^2 + e_{\mathrm{G}}^{-2}\dot{\epsilon_{\mathrm{II}}}^2) - \dot{\epsilon}_{\mathrm{I}}\right]. \tag{10}$$

Introducing $\Delta_{\mathrm{G}} = [\dot{\epsilon_{\mathrm{I}}}^2 + e_{\mathrm{G}}^{-2}\dot{\epsilon_{\mathrm{II}}}^2]^{1/2}$, Eq. (10) becomes

$$\alpha_r(\theta) = \frac{1}{2|\dot{\epsilon}|}\left[\frac{\Delta_G^2}{\Delta_{\mathrm{FG}}} - \dot{\epsilon}_{\mathrm{I}}\right]. \tag{11}$$

Assuming a normal flow rule (i.e., $e_{\mathrm{G}} = e_{\mathrm{F}}$), $\Delta_{\mathrm{G}} = \Delta_{\mathrm{FG}} = \Delta$ and Eq. (11) simplifies to $\alpha_r(\theta) = \frac{1}{2|\dot{\epsilon}|}[\Delta - \dot{\epsilon}_{\mathrm{I}}]$, which is Eq. (25) in Lipscomb et al. (2007), or Eq. (2) exactly. The formulation of $\alpha_r(\theta)$ in Eq. (11) is therefore a valid generalization of Eq. (2) for both normal and non-normal flow rules.

3.2 Coefficients for nonzero tensile strength

We build on the results of the previous section and consider a VP rheology with an elliptical yield curve, a non-normal flow rule, and nonzero tensile strength. With nonzero tensile strength and a non-normal flow rule, the stress invariants are expressed as

$$\sigma_{\mathrm{I}} = \zeta\dot{\epsilon}_{\mathrm{I}} - \frac{P_r(1-k_t)}{2}, \tag{12}$$

$$\sigma_{\mathrm{II}} = \eta\dot{\epsilon_{\mathrm{II}}}, \tag{13}$$

where k_t is a parameter that defines tensile strength (König Beatty and Holland, 2010), $\zeta = P_r(1+k_t)/2\Delta_{\mathrm{FG}}$, $\eta = e_{\mathrm{G}}^{-2}\zeta$, and Δ_{FG} is again equal to $(\dot{\epsilon_{\mathrm{I}}}^2 + e_{\mathrm{F}}^2 e_{\mathrm{G}}^{-4}\dot{\epsilon_{\mathrm{II}}}^2)^{1/2}$ (Ringeisen et al., 2021).

Eq. (24) in Wilchinsky et al. (2006) equates the work done by the internal stresses to the change in potential energy and the energy loss in opening (associated with tensile strength) and sliding. Neglecting the sliding term, this equation is

$$\sigma_{\mathrm{I}}\dot{\epsilon}_{\mathrm{I}} + \sigma_{\mathrm{II}}\dot{\epsilon_{\mathrm{II}}} = |\dot{\epsilon}|[\alpha_r(\theta)P_r + \alpha_o(\theta)P_o], \tag{14}$$

where P_o is the strength in opening (i.e., the tensile strength $k_t P_r$). In pure divergence ($\dot{\epsilon_{\mathrm{II}}} = 0$, $\dot{\epsilon}_{\mathrm{I}} > 0$, $\alpha_r = 0$), we have

$$\sigma_{\mathrm{I}}\dot{\epsilon}_{\mathrm{I}} = |\dot{\epsilon}|[\alpha_o(\theta = 0)P_o]. \tag{15}$$

Using Eq. (12), Eq. (15) can be written as

$$\left[\frac{P_r(1+k_t)|\dot{\epsilon}_{\mathrm{I}}|}{2|\dot{\epsilon}_{\mathrm{I}}|} - \frac{(1-k_t)P_r}{2}\right]|\dot{\epsilon}_{\mathrm{I}}| = |\dot{\epsilon}_{\mathrm{I}}|[\alpha_o(0)P_o], \tag{16}$$

which can be rearranged as

$$k_t P_r = P_o, \tag{17}$$

https://doi.org/10.5194/egusphere-2026-1362
Preprint. Discussion started: 11 May 2026

with $\alpha_o(0)$=1 (Moritz and Ukita, 2000).

We now consider the more general case with $\theta \neq 0$. Using Eqs. (12) and (13) and the definitions of ζ and η, Eq. (14) can be written as

$$\left[\frac{P_r(1+k_t)\dot{\epsilon_{\mathrm{I}}}}{2\Delta_{\mathrm{FG}}} - \frac{P_r(1-k_t)}{2}\right]\dot{\epsilon_{\mathrm{I}}} + e_{\mathrm{G}}^{-2}\frac{P_r(1+k_t)}{2\Delta_{\mathrm{FG}}}\dot{\epsilon_{\mathrm{II}}}^2 = |\dot{\epsilon}|[\alpha_r(\theta)P_r + \alpha_o(\theta)P_o], \tag{18}$$

which, with $P_o = k_t P_r$, can be rearranged as

$$\frac{1}{2|\dot{\epsilon}|}\left[(1+k_t)\frac{\Delta_{\mathrm{G}}^2}{\Delta_{\mathrm{FG}}} - (1-k_t)\dot{\epsilon_{\mathrm{I}}}\right] = \alpha_r(\theta) + \alpha_o(\theta)k_t. \tag{19}$$

With $\alpha_o = \alpha_r + \cos\theta$ (Thorndike et al., 1975) and $\cos\theta = \dot{\epsilon_{\mathrm{I}}}/|\dot{\epsilon}|$, we can write Eq. (19) as

$$\left[(1+k_t)\frac{\Delta_{\mathrm{G}}^2}{\Delta_{\mathrm{FG}}} - (1-k_t)\dot{\epsilon_{\mathrm{I}}}\right] = 2\alpha_r(1+k_t)|\dot{\epsilon}| + 2k_t\dot{\epsilon_{\mathrm{I}}}, \tag{20}$$

which gives an expression for the ridging coefficients:

$$\alpha_r = \frac{1}{2|\dot{\epsilon}|}\left[\frac{\Delta_{\mathrm{G}}^2}{\Delta_{\mathrm{FG}}} - \dot{\epsilon_{\mathrm{I}}}\right]. \tag{21}$$

This is the same expression we obtained earlier without tensile strength (i.e., $k_t = 0$). α_r and α_o are the same for $k_t = 0$ and $k_t > 0$ because for $k_t > 0$, the increase in the work done by the internal stresses and the increase in the energy dissipated are both proportional to k_t (not shown).

4 Conditions on e_{G} and e_{F}

The condition $0 \leq \alpha_r(\theta) \leq 1$ is a strict requirement (Thorndike et al., 1975) that places some restrictions on the choice of ellipse parameters e_F and e_G. We start with the condition that $\alpha_r(\theta) \geq 0$:

$$\alpha_r(\theta) = \frac{1}{2|\dot{\epsilon}|}\left[\frac{\Delta_{\mathrm{G}}^2}{\Delta_{\mathrm{FG}}} - \dot{\epsilon_{\mathrm{I}}}\right] \geq 0, \tag{22}$$

which can be rewritten as

$$\frac{\Delta_{\mathrm{G}}^2}{\Delta_{\mathrm{FG}}} \geq \dot{\epsilon_{\mathrm{I}}}. \tag{23}$$

This inequality is always satisfied in convergence (i.e., $\dot{\epsilon_{\mathrm{I}}} < 0$). However, if $\dot{\epsilon_{\mathrm{I}}} > 0$, the left hand side is not necessarily larger than $|\dot{\epsilon_{\mathrm{I}}}|$. Using the definitions of Δ_{G} and Δ_{FG}, we write

$$\left[\dot{\epsilon_{\mathrm{I}}}^2 + e_{\mathrm{G}}^{-2}\dot{\epsilon_{\mathrm{II}}}^2\right] \geq |\dot{\epsilon_{\mathrm{I}}}|\left[\dot{\epsilon_{\mathrm{I}}}^2 + e_{\mathrm{F}}^2 e_{\mathrm{G}}^{-4}\dot{\epsilon_{\mathrm{II}}}^2\right]^{1/2}, \tag{24}$$

https://doi.org/10.5194/egusphere-2026-1362
Preprint. Discussion started: 11 May 2026

which after squaring both sides can be rearranged as

$$\dot{\epsilon_{\mathrm{I}}}^2 \dot{\epsilon_{\mathrm{II}}}^2 \left(2e_{\mathrm{G}}^{-2} - e_{\mathrm{F}}^2 e_{\mathrm{G}}^{-4}\right) + e_{\mathrm{G}}^{-4} \dot{\epsilon_{\mathrm{II}}}^4 \geq 0. \tag{25}$$

Eq. (25) is satisfied if $\left(2e_{\mathrm{G}}^{-2} - e_{\mathrm{F}}^2 e_{\mathrm{G}}^{-4}\right) \geq 0$, which implies the condition

$$e_{\mathrm{G}} \geq \frac{e_{\mathrm{F}}}{\sqrt{2}}. \tag{26}$$

Second, we derive the condition for ensuring that $\alpha_r(\theta) \leq 1$:

$$\alpha_r(\theta) = \frac{1}{2|\dot{\epsilon}|}\left[\frac{\Delta_{\mathrm{G}}^2}{\Delta_{\mathrm{FG}}} - \dot{\epsilon_{\mathrm{I}}}\right] \leq 1, \tag{27}$$

which we rewrite as

$$\left(\Delta_{\mathrm{G}}^2 - \dot{\epsilon_{\mathrm{I}}}\Delta_{\mathrm{FG}}\right) \leq 2|\dot{\epsilon}|\Delta_{\mathrm{FG}}. \tag{28}$$

In the most difficult case, $\dot{\epsilon_{\mathrm{I}}} < 0$, Eq. (28) becomes

$$\left(\Delta_{\mathrm{G}}^2 + |\dot{\epsilon_{\mathrm{I}}}|\Delta_{\mathrm{FG}}\right) \leq 2|\dot{\epsilon}|\Delta_{\mathrm{FG}}. \tag{29}$$

Squaring both sides of Eq. (29) and rearranging terms, we obtain

$$2|\dot{\epsilon_{\mathrm{I}}}|\Delta_{\mathrm{G}}^2\Delta_{\mathrm{FG}} \leq 2\dot{\epsilon}_{\mathrm{I}}^4 + \left(4 + 3e_{\mathrm{F}}^2 e_{\mathrm{G}}^{-4} - 2e_{\mathrm{G}}^{-2}\right)\dot{\epsilon_{\mathrm{I}}}^2 \dot{\epsilon_{\mathrm{II}}}^2 + \left(4e_{\mathrm{F}}^2 e_{\mathrm{G}}^{-4} - e_{\mathrm{G}}^{-4}\right)\dot{\epsilon}_{\mathrm{II}}^4. \tag{30}$$

To obtain an analytical solution, we replace $|\dot{\epsilon_{\mathrm{I}}}|$ on the left-hand side of Eq. (30) by Δ_{FG}. As $|\dot{\epsilon_{\mathrm{I}}}| \leq \Delta_{\mathrm{FG}}$, this leads to a stricter condition on e_{G} and e_{F}. Moving all the terms to the right hand side leads to

$$0 \leq \left(4 - 4e_{\mathrm{G}}^{-2} + e_{\mathrm{F}}^2 e_{\mathrm{G}}^{-4}\right)\dot{\epsilon_{\mathrm{I}}}^2 \dot{\epsilon_{\mathrm{II}}}^2 + \left(4e_{\mathrm{F}}^2 e_{\mathrm{G}}^{-4} - e_{\mathrm{G}}^{-4} - 2e_{\mathrm{F}}^2 e_{\mathrm{G}}^{-6}\right)\dot{\epsilon}_{\mathrm{II}}^4. \tag{31}$$

This condition is always met if both terms on the right hand side are ≥ 0. For the first term, we can write

$$4e_{\mathrm{G}}^4 - 4e_{\mathrm{G}}^2 + e_{\mathrm{F}}^2 \geq 0, \tag{32}$$

which leads to the condition

$$e_{\mathrm{F}}^2 \geq 4\left(e_{\mathrm{G}}^2 - e_{\mathrm{G}}^4\right) = 4e_{\mathrm{G}}^2\left(1 - e_{\mathrm{G}}\right)\left(1 + e_{\mathrm{G}}\right). \tag{33}$$

This condition is satisfied for $e_{\mathrm{G}} > 1$, which makes the right-hand side negative. For $0 < e_{\mathrm{G}} \leq 1$, the condition can be simplified to

$$e_{\mathrm{F}} \geq 2\sqrt{e_{\mathrm{G}}^2 - e_{\mathrm{G}}^4}. \tag{34}$$

https://doi.org/10.5194/egusphere-2026-1362
Preprint. Discussion started: 11 May 2026

which only excludes values of e_F to the left of the green curve in Figure 1. Multiplying by e_G^4, the second term in Eq. (31) becomes

$$4e_\mathrm{F}^2 - 1 - 2e_\mathrm{F}^2 e_\mathrm{G}^{-2} \geq 0, \tag{35}$$

which after a few manipulations leads to the last condition:

$$e_\mathrm{F} \geq \frac{e_\mathrm{G}}{\sqrt{2(2e_\mathrm{G}^2 - 1)}}. \tag{36}$$

The conditions given by Eq. (26), Eq. (34), and Eq. (36) are combined graphically in Fig. (1). Note that Eq. (36) also implies the condition $e_\mathrm{G} > \frac{1}{\sqrt{2}}$. For a normal flow rule (i.e., $e_\mathrm{G} = e_\mathrm{F} = e$), these conditions are always respected for $e \geq 1$.

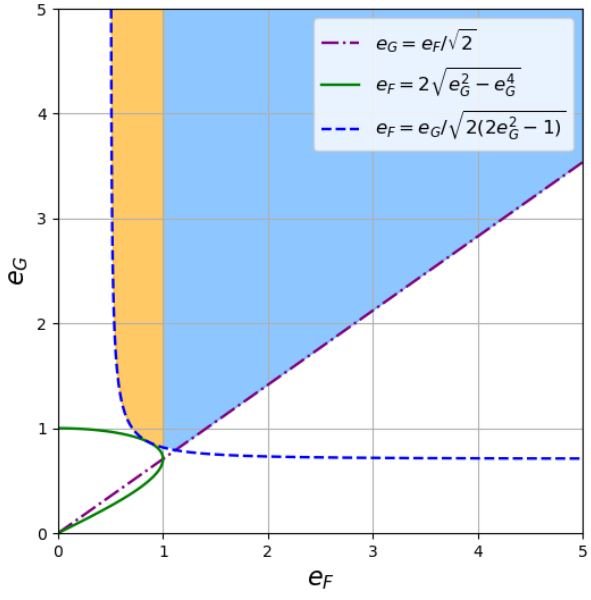

Figure 1. The blue and orange regions display the pairs of e_F and e_G that lead to bounded values of α_o and α_r between 0 and 1. As sea ice models usually have $e_\mathrm{F} > 1$, the blue region is really the region of interest.

5 Incorrect formulations of opening and ridging coefficients

The correct (CORR) formulation and the main contribution of this article is given by Eq. (21). It is repeated here for comparison with the other formulations presented:

$$\alpha_r = \frac{1}{2|\dot{\epsilon}|}\left[\frac{\Delta_\mathrm{G}^2}{\Delta_\mathrm{FG}} - \dot{\epsilon}_\mathrm{I}\right]. \tag{37}$$

https://doi.org/10.5194/egusphere-2026-1362
Preprint. Discussion started: 11 May 2026

A first study of the impact of an elliptical yield curve and a non-normal flow rule on simulated sea ice in realistic pan-Arctic experiments used an incorrect expression of α_r (Lemieux et al., 2025). Instead of the correct formulation (Eq. 21), the formulation for a VP rheology with normal flow rule (Eq. 2) was modified by replacing Δ by Δ_{FG}. This incorrect formulation, referred to as INC1, is then

$$\alpha_r = \frac{1}{2|\dot{\epsilon}|}\left[\Delta_{\mathrm{FG}} - \dot{\epsilon}_{\mathrm{I}}\right]. \tag{38}$$

We introduce another potentially incorrect formulation by expressing Δ only with the yield curve parameter e_{F}. With this second incorrect formulation, referred to as INC2, α_r becomes

$$\alpha_r = \frac{1}{2|\dot{\epsilon}|}\left[\Delta_{\mathrm{F}} - \dot{\epsilon}_{\mathrm{I}}\right], \tag{39}$$

with $\Delta_{\mathrm{F}} = [\dot{\epsilon_{\mathrm{I}}}^2 + e_{\mathrm{F}}^{-2}\dot{\epsilon_{\mathrm{II}}}^2]^{1/2}$.

Note that all these formulations are correct and equivalent for a normal flow rule (i.e., $e_{\mathrm{F}} = e_{\mathrm{G}}$). We use these methods to assess the impact of the incorrect coefficients in Lemieux et al. (2025) and to evaluate the sensitivity of simulated sea ice to the formulation of the opening and ridging coefficients when using a non-normal flow rule.

6 Experimental setup

We use the same experimental setup as in Lemieux et al. (2025). Some information is provided here but more details can be found in Section 3 in Lemieux et al. (2025). The setup is based on the NEMOv3.6 ocean model (Madec, 2008) and the CICEv6.5.0 sea ice model (Hunke et al., 2023), augmented to include the new formulation for the ridging and opening coefficients. We use here 10 ice thickness categories based on the scheme of Lipscomb (2001) with boundaries between categories at 10, 15, 30, 50, 70, 120, 200, 400 and 600 cm (see also Smith et al., 2016).

The regional domain covers the Arctic, the North Pacific and the North Atlantic. The grid has a spatial resolution of 1/12° (4-5 km in the central Arctic). The B-grid discretization is used for CICE.

The spinup procedure is also described in Section 3 in Lemieux et al. (2025). The spinup solution on 25 September 2004 is the restart that was used for all the simulations in this article. The simulations, forced by ECCC atmospheric reforecasts (Smith et al., 2014), end on 1 October 2010.

https://doi.org/10.5194/egusphere-2026-1362
Preprint. Discussion started: 11 May 2026

exp	e_{F}	e_{G}	method
CORRa	1.75	1.25	CORR
INC1a	1.75	1.25	INC1
INC2a	1.75	1.25	INC2
CORRb	1.75	1.75	CORR
CORRc	1.75	2.63	CORR

Table 1. List of numerical experiments with values of e_{F}, e_{G} and the method used for the ridging and opening coefficients.

7 Numerical experiments

We conducted a series of numerical experiments to study the impact of the ridging and opening coefficients on the simulated sea ice. As this study follows our work in Lemieux et al. (2025), we repeated some simulations with the same values of e_{G} and e_{F}. To limit the number of experiments, all of them use $e_{\mathrm{F}} = 1.75$. Again, we used $e_{\mathrm{G}} = 1.75$ and $e_{\mathrm{G}} = 2.63$. However, $e_{\mathrm{G}} = 1.16$ does not meet the conditions derived in Sect. 4 (i.e., the pair of $e_{\mathrm{F}} = 1.75, e_{\mathrm{G}} = 1.16$ lies outside the blue region in Fig. 1). We therefore tested the value $e_{\mathrm{G}} = 1.25$. Table 1 lists the different experiments with the values of e_{F}, e_{G} and the method for the ridging and opening coefficients.

The most important experiments in this article are CORRa, INC1a and INC2a. They show the impact of the formulation of the ridging and opening coefficients on the sea ice cover when using a non-normal flow rule. CORRb and CORRc are two additional experiments, which use the correct ridging and opening coefficients (CORR), to compare with the results of Lemieux et al. (2025).

Fig. 2 displays the values of the ridging coefficients α_r and α_o as a function of the angle θ for experiments CORRa, INC1a and INC2a. It indicates that the incorrect method (INC1) used by Lemieux et al. (2025) implies a more active redistribution function (for both opening and ridging). The other incorrect formulation (INC2) is close to CORR and should lead to a similar sea ice cover.

Fig. 3 displays the total sea ice volume as a function of time over the whole period of the simulations. As suggested by Fig. 2, the total volume with the INC2 formulation (Fig. 3a) is very similar to that with CORR (the blue line is hidden behind the violet one). In contrast, the incorrect formulation INC1 notably impacts the simulated sea ice cover. The volume is clearly larger with INC1 than with CORR.

Fig. 3b shows the impact of the plastic potential parameter e_{G} when keeping e_{F} fixed and using the CORR formulation. Consistent with the results of Lemieux et al. (2025), reducing e_{G} increases the total volume. However, Fig. 3a indicates that the incorrect formulation (INC1) used by Lemieux et al. (2025) exacerbates this effect.

https://doi.org/10.5194/egusphere-2026-1362
Preprint. Discussion started: 11 May 2026

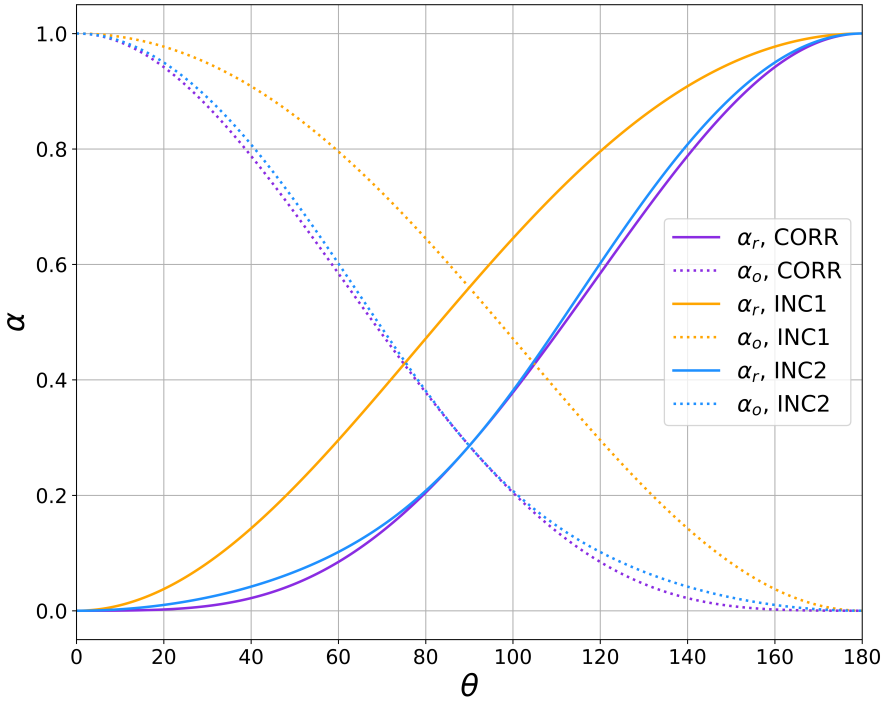

Figure 2. Ridging (solid lines) and opening (dotted lines) coefficients for $e_{\mathrm{F}} = 1.75$ and $e_{\mathrm{G}} = 1.25$ as a function of the angle θ. The correct formulation is in violet while INC1 is in orange and INC2 is in blue.

The thicker ice cover with INC1 compared to CORR is ubiquitous (Fig. 4a). On the other hand, INC2 leads to smaller and less systematic differences compared to CORR. We attribute these differences in thickness to the fact that compared to the CORR formulation, INC1 enhances the opening in the sea ice cover and therefore favors the growth of sea ice in winter and melt in summer. To verify this, we calculated the daily average concentration and the total growth (in km^3) in the central Arctic for experiments CORRa, INC1a and INC2a. These quantities were calculated in the region defined by the pack ice mask used by Lemieux et al. (2025) (see their Fig.1). The average concentration with INC1 is almost always smaller than the one obtained with CORR (Fig. 5a). The smaller concentration with INC1 leads to enhanced growth in winter and increased melt during summer (Fig. 5b). Differences in concentration and growth between INC2a and CORRa are close to zero over the whole period of the simulations. We note that the agreement between INC2a and CORRa is coincidental and depends on the chosen values of e_{F} and e_{G}. Other combinations of these parameters lead to opening and ridging coefficients that further deviate from the ones obtained with CORR (not shown).

The shapes of ITDs also help to understand the impact of the different formulations of the opening and ridging coefficients. The mean and spatially averaged ITD for CORRa (Fig. 6a) exhibits a mode at category seven and has little ice in thin categories. With its more active redistribution function (for both opening and ridging), INC1a enhances the fraction of open water and

https://doi.org/10.5194/egusphere-2026-1362
Preprint. Discussion started: 11 May 2026

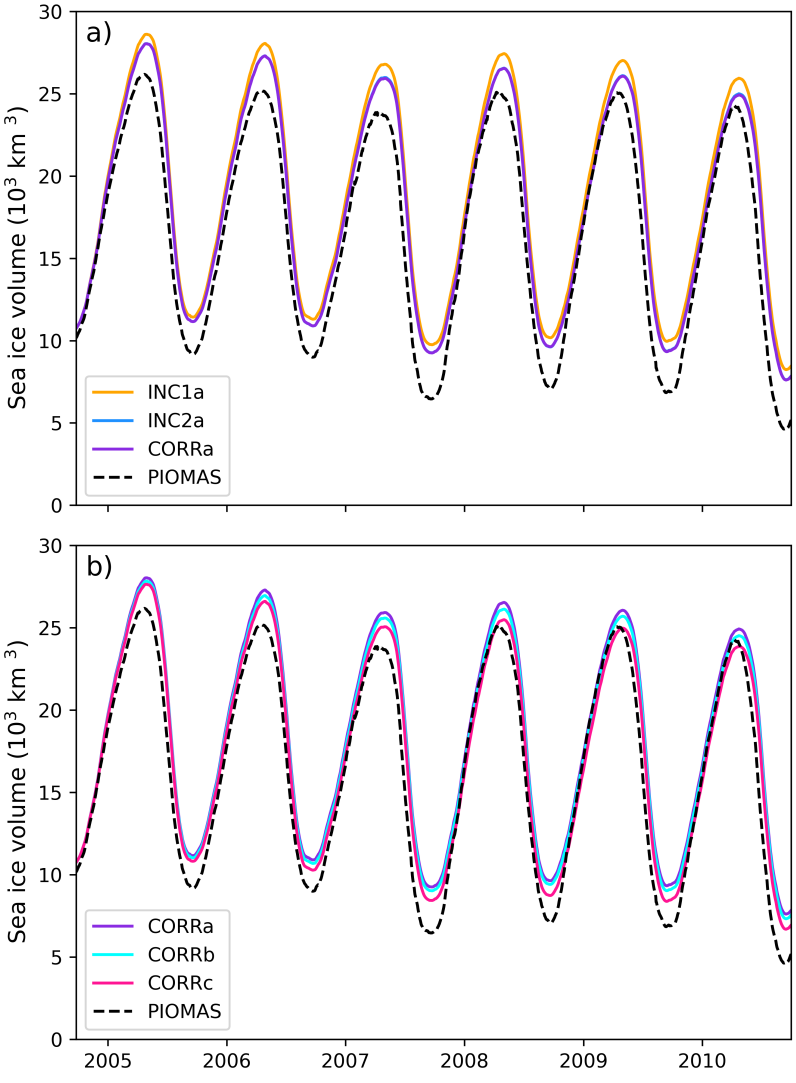

Figure 3. Total simulated daily mean sea ice volume as a function of time for the different methods (a) and for different values of e_G with the correct method (b). As a reference, the dashed black line shows the sea ice volume simulated by the PIOMAS system. The blue line (INC2a) in panel (a) is not visible because the violet one (CORRa) is on top of it.

the partial concentrations for thin categories and redistributes more ice in the thickest categories (8-10). The ITD for INC2a closely resembles the one of CORRa (not shown).

https://doi.org/10.5194/egusphere-2026-1362
Preprint. Discussion started: 11 May 2026

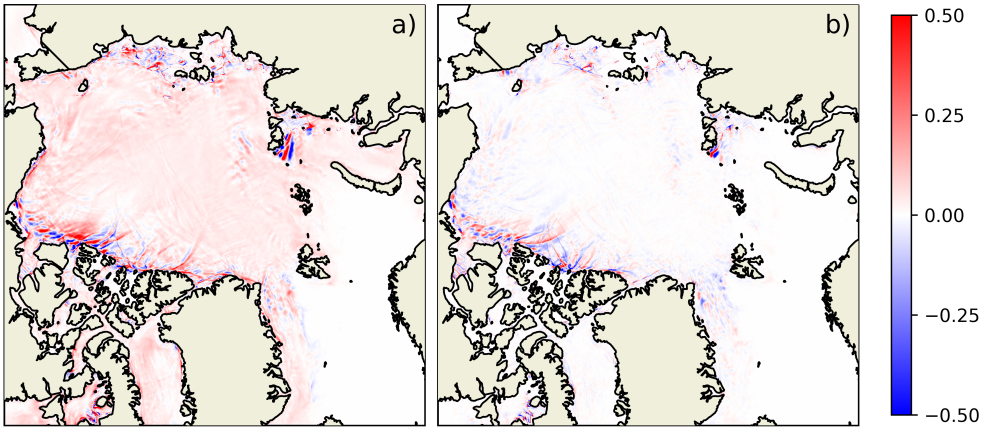

Figure 4. Differences in mean thicknesses (m) over the period February 1 to April 30 2005. (a) INC1a minus CORRa and (b) INC2a minus CORRa.

8 Discussion and concluding remarks

We introduced a general formulation for the ridging and opening coefficients of the redistribution function that are valid for an elliptical yield curve with either a normal or a non-normal flow rule. These new coefficients reduce to the standard ones in the case of a normal flow rule. Moreover, we showed that the ridging and opening coefficients remain the same when adding tensile strength. We recommend to examine the range of validity of the ridging and opening coefficients for each new rheology, as our results are specific to elliptic yield curves and plastic potentials. For example, the situation may be different for the Mohr–Coulomb yield curves (Tremblay and Mysak, 1997). For the teardrop and parabolic lens yield curves with a normal flow rule (Zhang and Rothrock, 2005; Ringeisen et al., 2023), the correct formulation is given in Zhang and Rothrock (2005, their App. B).

Further, the range of valid values of e_{G} and e_{F} (Fig. 1) is constrained by the condition that the ridging and opening coefficients are bounded by 0 and 1. Neglecting this constraint leads to unrealistic values of the coefficients (Fig. 7). For $e_{\mathrm{F}} = 2$ and $e_{\mathrm{G}} = 1.1$, α_r and α_o are negative over a range of θ. This is unrealistic. For example, $\alpha_r < 0$ implies a redistribution of sea ice from thick categories to thin ones (i.e., it would cause 'unridging'). A normal flow rule with $e_{\mathrm{F}} = e_{\mathrm{G}} \geq 1$ always leads to coefficients that are bounded by 0 and 1. However, our results demonstrate that ridging and opening coefficients could be unrealistic when $e_{\mathrm{F}} = e_{\mathrm{G}} < 1$. The red curves in Fig. 7 provides an example of unrealistic ridging and opening coefficients with $e_{\mathrm{F}} = e_{\mathrm{G}} = 0.6$. With this pair of e_{F} and e_{G}, the coefficients are larger than 1 over a range of θ and are maximum at intermediate θ rather than at $\theta = 0°$ (for α_o in pure divergence) and $\theta = 180°$ (for α_r in pure convergence). We therefore advise that multi-category models should be used carefully with ellipse ratios $e_{\mathrm{F}} = e_{\mathrm{G}} < 1$ (e.g., Miller et al., 2005). More generally, Figure 1 provides recommendations for choosing valid pairs $(e_{\mathrm{F}}, e_{\mathrm{G}})$.

https://doi.org/10.5194/egusphere-2026-1362
Preprint. Discussion started: 11 May 2026

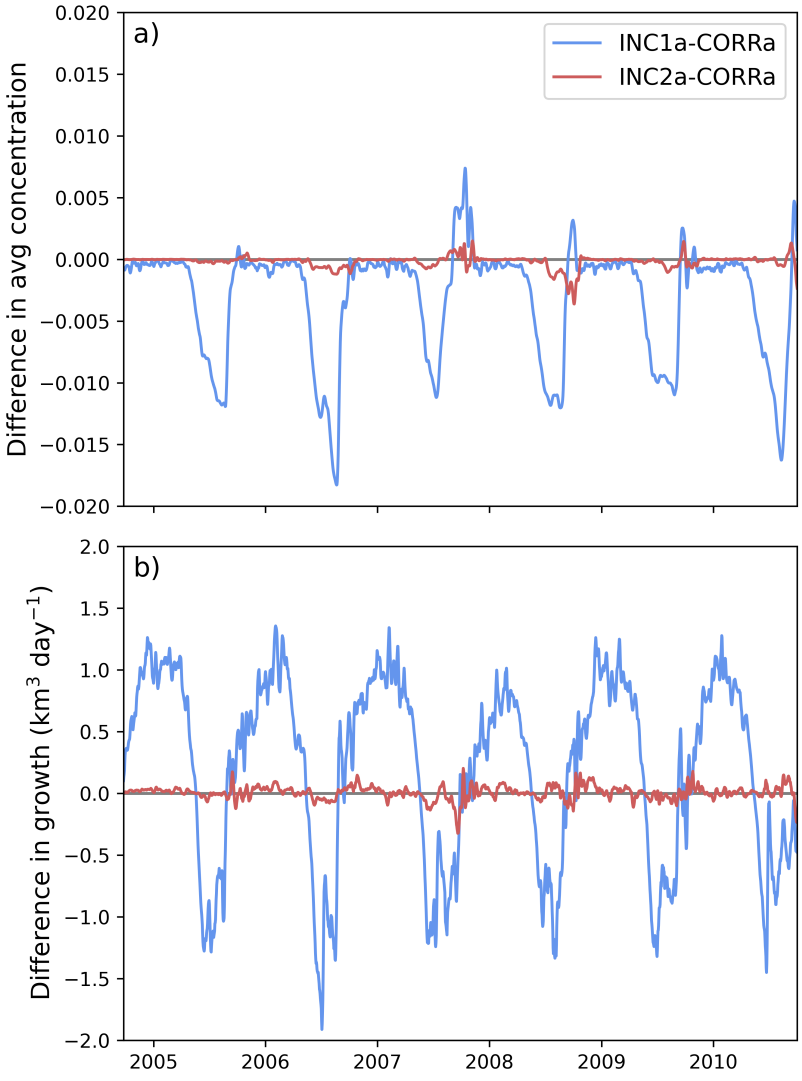

Figure 5. Difference in the average concentration between INC1a and CORRa (in blue) and between INC2a and CORRa (in red) (a) and difference in the daily growth between INC1a and CORRa (in blue) and between INC2a and CORRa (in red). These quantities were calculated in region defined by a pack ice mask. A seven-day rolling mean was applied to the time series. $e_{\mathrm{F}} = 1.75$ and $e_{\mathrm{G}} = 1.25$ for all these experiments.

https://doi.org/10.5194/egusphere-2026-1362
Preprint. Discussion started: 11 May 2026

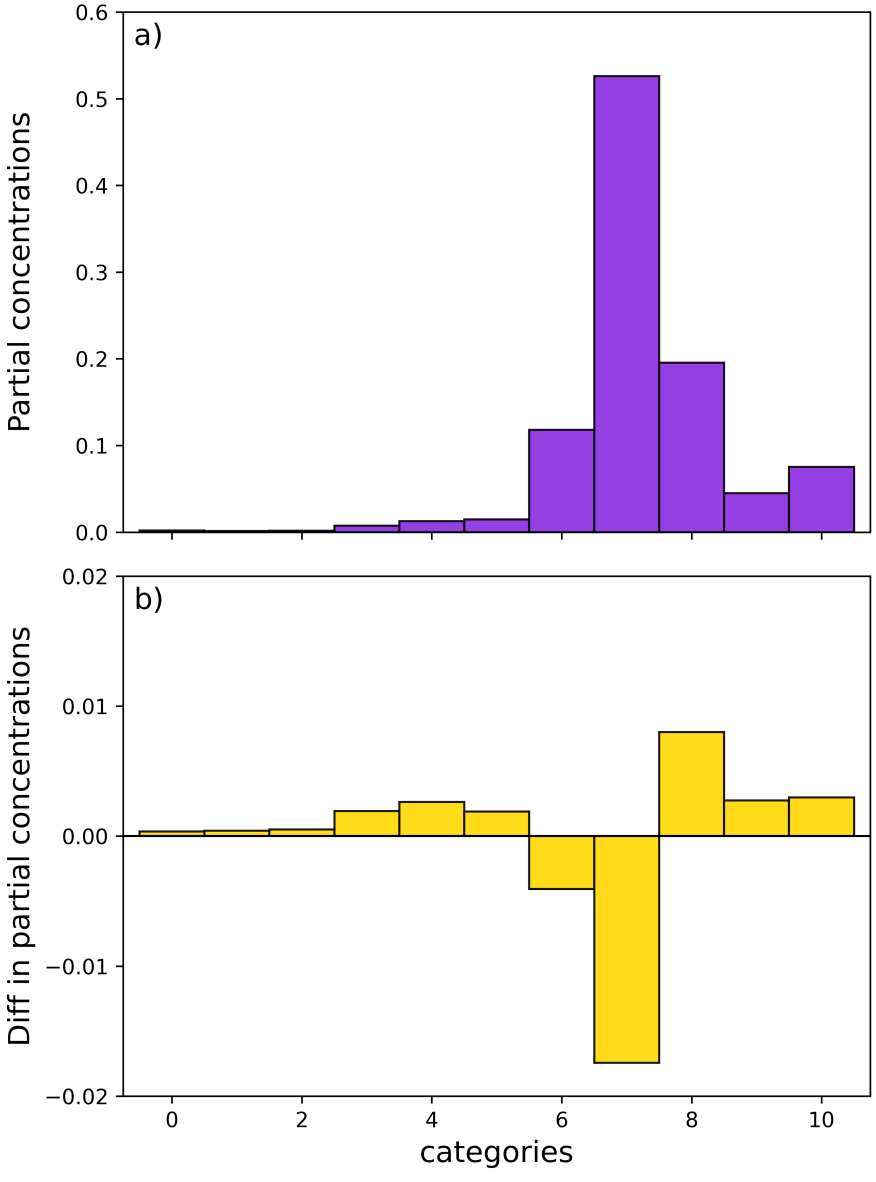

Figure 6. Mean and spatially averaged ITD for CORRa (a). Difference (INC1a-CORRa) between the mean and spatially averaged ITDs (b). The means are calculated from spatial averages over the period February 1 to April 30 2005. The spatial averages are calculated in a region defined by a pack ice mask. Note that the ITDs include the amount of open water (category 0).

https://doi.org/10.5194/egusphere-2026-1362
Preprint. Discussion started: 11 May 2026

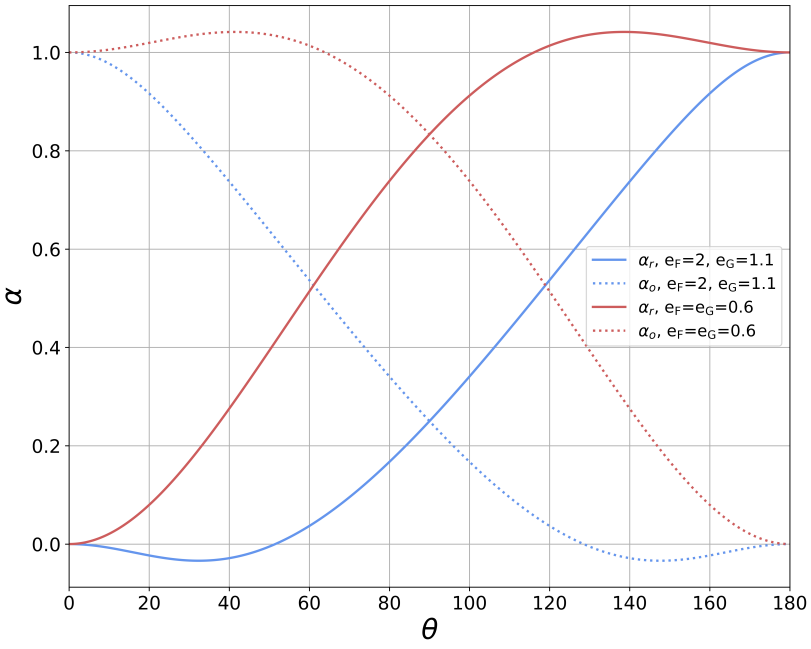

Figure 7. Ridging (solid lines) and opening (dotted lines) coefficients calculated with the CORR formulation for $e_{\mathrm{F}} = 2$ and $e_{\mathrm{G}} = 1.1$ (non-normal flow rule, in blue) and for $e_{\mathrm{F}} = 0.6$ and $e_{\mathrm{G}} = 0.6$ (normal flow rule, in red) as a function of the angle θ.

https://doi.org/10.5194/egusphere-2026-1362
Preprint. Discussion started: 11 May 2026

Code and data availability.

Release 6.5.0 of the CICE sea ice model was used for the simulations of this article. It can be obtained at https://github.com/CICE-Consortium/CICE/ releases/tag/CICE6.5.0 (last access: 5 March 2026) and on Zenodo at https://doi.org/10.5281/zenodo.10056499 (Hunke et al., 2023). Release 6.5.0 includes Icepack 1.4.0. Modified code for the formulations of the ridging coefficients can be found at https://zenodo.org/records/18894501. The PIOMAS sea ice volume dataset can be obtained at https://psc.apl.uw.edu/research/projects/arctic-sea-ice-volume-anomaly/data (last access: 5 March 2026).

Author contributions. JFL and DR derived the equations. JFL implemented the new opening and ridging coefficients in CICE. JFL designed and ran the numerical experiments. JFL wrote the article with contributions from all the co-authors.

Competing interests. no competing interests are present

Acknowledgements. JFL thanks his colleagues at the Canadian Centre for Meteorological and Environmental Prediction (CCMEP) for CICE-NEMO model development and their help with the numerical experiments. WHL was supported by the NSF National Center for Atmospheric Research, which is a major facility sponsored by the National Science Foundation (NSF) under Cooperative Agreement no. 1852977.

https://doi.org/10.5194/egusphere-2026-1362
Preprint. Discussion started: 11 May 2026

References

Coon, M. D., Maykut, G. A., Pritchard, R. S., Rothrock, D. A., and Thorndike, A. S.: Modeling the pack ice as an elastic-plastic material, AIDJEX Bulletin, 24, 1–105, 1974.

Hibler, W. D.: A dynamic thermodynamic sea ice model, J. Phys. Oceanogr., 9, 815–846, 1979.

Hunke, E., Allard, R., Bailey, D. A., Blain, P., Craig, A., Dupont, F., DuVivier, A., Grumbine, R., Hebert, D., Holland, M., Jeffery, N., Lemieux, J.-F., Osinski, R., Rasmussen, T., Ribergaard, M., Roach, L., Roberts, A., Turner, M., Winton, M., and Worthen, D.: CICE-Consortium/CICE: CICE Version 6.5.0, https://doi.org/10.5281/zenodo.10056499, 2023.

Itkin, P., Losch, M., and Gerdes, R.: Landfast ice affects the stability of the Arctic halocline: evidence from a numerical model, J. Geophys. Res., 120, 2622–2635, https://doi.org/10.1002/2014JC010353, 2015.

König Beatty, C. and Holland, D. M.: Modeling landfast sea ice by adding tensile strength, J. Phys. Oceanogr., 40, 185–198, https://doi.org/10.1175/2009JPO4105.1, 2010.

Lemieux, J.-F., Dupont, F., Blain, P., Roy, F., Smith, G. C., and Flato, G. M.: Improving the simulation of landfast ice by combining tensile strength and a parameterization for grounded ridges, J. Geophys. Res. Oceans, 121, 7354–7368, https://doi.org/10.1002/2016JC012006, 2016.

Lemieux, J.-F., Plante, M., Hutter, N., Ringeisen, D., Tremblay, B., Roy, F., and Blain, P.: Impact of non-normal flow rule on linear kinematic features in pan-Arctic ice-ocean simulations, EGUsphere, 2025, 1–33, https://doi.org/10.5194/egusphere-2024-3831, 2025.

Lipscomb, W.: Remapping the thickness distribution in sea ice models, J. Geophys. Res., 106, 13,989–14,000, 2001.

Lipscomb, W. H., Hunke, E. C., Maslowski, W., and Jakacki, J.: Ridging, strength, and stability in high-resolution sea ice models, J. Geophys. Res., 112, https://doi.org/10.1029/2005JC003355, 2007.

Madec, G.: NEMO ocean engine, Note du Pôle de modélisation, Institut Pierre-Simon Laplace (IPSL), France, No 27, ISSN No 1288-1619, 2008.

Miller, P. A., Laxon, S. W., and Feltham, D. L.: Improving the spatial distribution of modeled Arctic sea ice thickness, Geophys. Res. Lett., 32, L18 503, 2005.

Moritz, R. E. and Ukita, J.: Geometry and the deformation of pack ice: I. A simple kinematic model, Annals of Glaciology, 31, 313–322, 2000.

Ringeisen, D., Tremblay, L. B., and Losch, M.: Non-normal flow rules affect fracture angles in sea ice viscous–plastic rheologies, The Cryosphere, 15, 2873–2888, https://doi.org/10.5194/tc-15-2873-2021, 2021.

Ringeisen, D., Losch, M., and Tremblay, L. B.: Teardrop and Parabolic Lens Yield Curves for Viscous-Plastic Sea Ice Models: New Constitutive Equations and Failure Angles, Journal of Advances in Modeling Earth Systems, 15, e2023MS003 613, https://doi.org/10.1029/2023MS003613, _eprint: https://onlinelibrary.wiley.com/doi/pdf/10.1029/2023MS003613, 2023.

Rothrock, D. A.: The Energetics of the Plastic Deformation of Pack Ice by Ridging, Journal of Geophysical Research, 80, 4514–4519, 1975.

Smith, G. C., Roy, F., Mann, P., Dupont, F., Brasnett, B., Lemieux, J.-F., Laroche, S., and Bélair, S.: A new atmospheric dataset for forcing ice-ocean models: evaluation of reforecasts using the Canadian global deterministic prediction system, Q. J. R. Meteorol. Soc., 140, 881–894, https://doi.org/10.1002/qj.2194, 2014.

Smith, G. C., Roy, F., Reszka, M., Surcel Colan, D., He, Z., Deacu, D., Belanger, J.-M., Skachko, S., Liu, Y., Dupont, F., Lemieux, J.-F., Beaudoin, C., Tranchant, B., Drevillon, M., Garric, G., Testut, C.-E., Lellouche, J.-M., Pellerin, P., Ritchie, H., Lu, Y., Davidson, F.,

https://doi.org/10.5194/egusphere-2026-1362
Preprint. Discussion started: 11 May 2026

Buehner, M., Caya, A., and Lajoie, M.: Sea ice forecast verification in the Canadian Global Ice Ocan Preduction Sesteem, Quarterly Journal of the Royal Meteorological Society, 142, 659–671, https://doi.org/10.1002/qj.2555, 2016.

Stern, H. L., Rothrock, D. A., and Kwok, R.: Open water production in Arctic sea ice: Satellite measurements and model parameterizations, J. Geophys. Res., 100, 20 601–20 612, 1995.

Thorndike, A. S., Rothrock, D. A., Maykut, G. A., and Colony, R.: The thickness distribution of sea ice, J. Geophys. Res., 80, 4501–4513, 1975.

Tremblay, L. B. and Mysak, L. A.: Modeling sea ice as a granular material, including the dilatancy effect, J. Phys. Oceanogr., 27, 2342–2360, 1997.

Ukita, J. and Moritz, R. E.: Yield curves and flow rules of pack ice, Journal of Geophysical Research: Oceans, 100, 4545–4557, 1995.

Van Achter, G., Fichefet, T., Goosse, H., Pelletier, C., Sterlin, J., Huot, P.-V., Lemieux, J.-F., Fraser, A., Haubner, K., and Porter-Smith, R.: Modelling landfast sea ice and its influence on ocean-ice interactions in the area of the Totten Glacier, East Antarctica, Ocean Modelling, 169, 101 920, https://doi.org/https://doi.org/10.1016/j.ocemod.2021.101920, 2022.

Wilchinsky, A. V., Feltham, D. L., and Miller, P. A.: A multithickness sea ice model accounting for sliding friction, Journal of physical oceanography, 36, 1719–1738, 2006.

Zhang, J. and Rothrock, D. A.: Effect of sea ice rheology in numerical investigations of climate, J. Geophys. Res., 110, C08 014, doi:10.1029/2004JC002599, 2005.